Radiofrequency Current Drive Experiments in MST *

J. K. Anderson 1), D. R. Burke 1), S. J. Diem 2), C. B. Forest 1), J. A. Goetz 1), A. H. Seltzman 1)

1) Department of Physics, University of Wisconsin, Madison, WI, USA
2) Oak Ridge National Laboratory, Oak Ridge, TN, USA

Email of main author: jkanders@wisc.edu

Abstract. Current profile control is a crucial tool for understanding the drive of tearing fluctuations in the reversed field pinch. Simulations of auxiliary edge parallel current drive predict a reduction of tearing activity, and indeed in experiment there is a significant decrease of magnetic fluctuations with inductive edge current drive in the MST. This in turn leads to a dramatically increased (factor of 10) electron energy confinement time and evidence that transport is no longer dominated by magnetic turbulence. The use of rf waves to drive edge current offers steady and more precise profile control than the existing inductive approach, which is transient, radially diffuse and induces a large change to the magnetic equilibrium. Lower Hybrid (LH) and electron Bernstein waves (EBW) are being studied as candidates for the overdense, high beta plasma. Ray tracing and Fokker-Planck calculations predict good absorption and directional control for both waves, as required for effective current drive. The lower hybrid studies involve novel antenna design and extending LH physics to plasmas with high dielectric constant. In contrast, the EBW studies benefit from simpler antenna requirements, but the mode conversion wave physics needs to be established for a high beta RFP plasma. At present, localized x-ray emission has been observed with rf injection at the 100kW level of each wave. Toroidally localized hard x-ray (HXR) emission with energy as high as 50keV is observed during LH injection (with $\sim$125 kW coupled to the plasma). The flux and energy spectrum is consistent with acceleration of plasma electrons in the antenna near field with electric fields computed by electromagnetic modeling. Enhanced SXR emission (4-7 keV) is observed during EBW injection ($\sim$100kW of 3.6GHz launched) when accompanied by a period of low magnetic fluctuations. Hardware for the EBW current drive project is being upgraded to use a 1MW, 5.5 GHz klystron, with the higher frequency (shorter wavelength) enabling the use of a smaller port hole for the launching antenna.

1. Introduction

Development of non-inductive current drive techniques for the RFP is important as both a scientific tool and a way to advance the performance of the confinement scheme. Energy transport in the core of conventional RFP plasmas results from parallel losses along stochastic magnetic field lines that wander from the core to the edge. The low safety factor in the RFP permits many possible resonant surfaces for resistive MHD tearing, the origin of the dominant magnetic fluctuations. In standard RFP plasmas, i.e., those formed by steady toroidal induction, a spectrum of modes arises through linear tearing instability from current profile peaking and subsequent nonlinear mode coupling. These modes produce numerous overlapping magnetic islands, resulting in a stochastic magnetic topology that in turn produces rapid radial transport. Peaking of the parallel current profile and subsequent tearing instability is in large part a consequence of the chosen means of current drive. For toroidal induction, the parallel component of the electric field is centrally peaked, primarily because the poloidal field is dominant in the outer region of the plasma. This tends to drive a peaked current profile which is unstable to MHD tearing. When tearing instability sets in, nonlinear interaction creates a dynamo emf that

*This work supported by the US DOE.

limits the peaking of the current profile. This is a strong effect, producing a net parallel current everywhere in the edge region and maintaining the current profile near marginal stability. The dynamo-driven current also provides the poloidal current necessary to maintain toroidal magnetic field reversal. Hence, the formation and maintenance of the RFP equilibrium is self-organized and strongly coupled to energy transport.
Inductive current profile control has been highly successful in reducing transport in MST, but it is thus far transient and non-localized. The optimal current profile control technique for RFP plasmas is expected to be rf generated as it offers the possibility of steady and precise modification. Two separate rf experiments are under development in an attempt to drive auxiliary current in the high beta plasma of the MST by launching electrostatic waves. The electron Bernstein wave is excited by launch of an electromagnetic wave at the plasma edge and can drive current at the electron cyclotron resonance layer. A lower hybrid current drive scheme is also being developed, where an interdigital line antenna launches the slow wave at the plasma boundary. In this paper, we report localized xray emission during both rf injection techniques and outline next steps for each experiment.

2. Electron Bernstein Wave

EBW heating and current drive has been demonstrated in the stellarator, tokamak, and spherical torus as cited in [1] [2] [3] and others. The RFP presents unique challenges to rf heating and current drive. The plasma is very over dense, with $\omega_{pe} > \omega_{ce}$ within a few cm of the plasma boundary. The low magnetic field strength in the MST places the ECRF in the microwave range: rf power is readily available and the well-established tokamak lower hybrid grill can be used, however the relatively low frequency leads to larger characteristic antenna size which is a technical challenge where the close-fitting conducting shell (limited port size) is essential to equilibrium. Wave launching structures for experiments on MST must fit through an 11.5 cm diameter circular port.
A staged experimental approach is underway toward EBW current drive on MST. First, EBE measured (10^{-8} W) from the overdense plasma established the reciprocal mode-conversion process takes place [4]. A phased waveguide grill has been shown to couple launched rf (at 10^{1} W) to the EBW with adequate efficiency [5]. Heating experiments at 10^{5} W have shown localized soft xray enhancement, with rf heating power still an order of magnitude less than the background Ohmic input power. Development of a significant heating experiment, with source power of 10^{6} W is underway.

Figure 1 is an illustration of a 20 chord SXR diagnostic and its location with respect to the EBW antenna. The MST poloidal cross section (minor radius 0.52m) is sketched, with the waveguide antenna shown on the outboard edge. The camera (courtesy of collaboration with Consorzio-RFX) installed at the same toroidal angle views vertically downward. The camera consists of a 400 μm Be filter in front of a 35 μm Si photodiode which restricts the measured emission to about 4-7 keV. The outboard chords of the camera intersect the Genray predicted path of the EBW shown as the green line. The target plasma is a discharge with 250 kA of plasma current, an central magnetic field of about .25T, an edge magnetic field of about .1T, a line-average density of about 1x10^{13} cm^{-3}, and central electron temperature of about 500 eV. The antenna is oriented to excite the X-mode at the plasma boundary and mode conversion to the EBW takes place within a few cm. Coupling to the EBW, as inferred by measuring the ratio of reflected to launched power, is typically around 75 to 80%. The EBW then propagates to the doppler-shifted electron cyclotron resonance where its power is deposited. Optimal coupling to

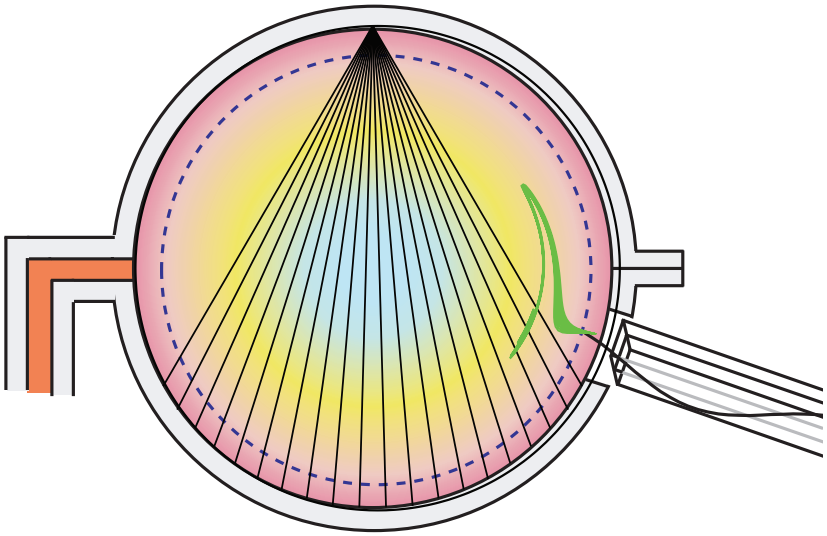

FIG. 1. 20 chord pinhole camera monitoring SXR emission at the same toroidal angle as the EBW antenna. The green line is the Genray ray tracing result for a 3.6 GHz Bernstein wave launched in the target plasma.

the plasma requires particular phasing of the waveguide grill. Further, a boron nitride dielectric endcap is on the antenna acting as a limiter and preventing plasma from contacting the copper antenna.

Recent measurements confirm an increase of soft x-ray emission (4-7 keV) is caused by rf injection but the mechanism responsible for x-ray production is still under investigation. Figure 2 is a plot of some relevant signals with time. Rf power is injected from 18 to 24 msec during the discharge. The top line in Fig. 2a is the sum of net (forward minus reflected) power in the four waveguide arms leading to the antenna, totaling about 80 kW at its maximum and is surmised to go into the Bernstein mode. The 500 μs dropout in power at 21.5 ms is a programmed modulation to investigate rf turn off effects; the drop in power at t= 23.2 msec is an indication of imperfect antenna behavior. The measured soft x-ray signal (Fig. 2b) on chord 19 (second from the outboard edge) is coincident with rf injection. The m=0 mode activity (Fig. 2c) demonstrates that measurable 4-7 keV emission requires both rf injection and electron confinement (bursts in the m=0 activity correspond to rapid confinement loss). This consequence is loosely predicted by Fokker-Plank modeling where increasing radial diffusion in the code from $\sim$zero to 100 m^2/s decreases the predicted emission.

The time evolution of the SXR signal illustrates the effect of the rf on emission. From an experimental point of view it is convenient that there is effectively zero background emission: no signal when the rf is off. Coincident with rf turn-on the SXR emission becomes measurable. (The brief drop of signal in the first 100 μs of injection is likely an indication of imperfect antenna operation). As the antenna delivers power, the SXR emission remains quite high (arbitrary units, but orders of magnitude above the noise level). At the programmed gate (21.5 to 22 ms) the emission goes quickly to zero. The final drop in SXR emission at 23.2 msec is coincident with the malfunction (arc) where the forward power notably drops and the net injected power becomes low.

After the rf resumes (following the programmed gate) at 22 ms, the SXR emission is large

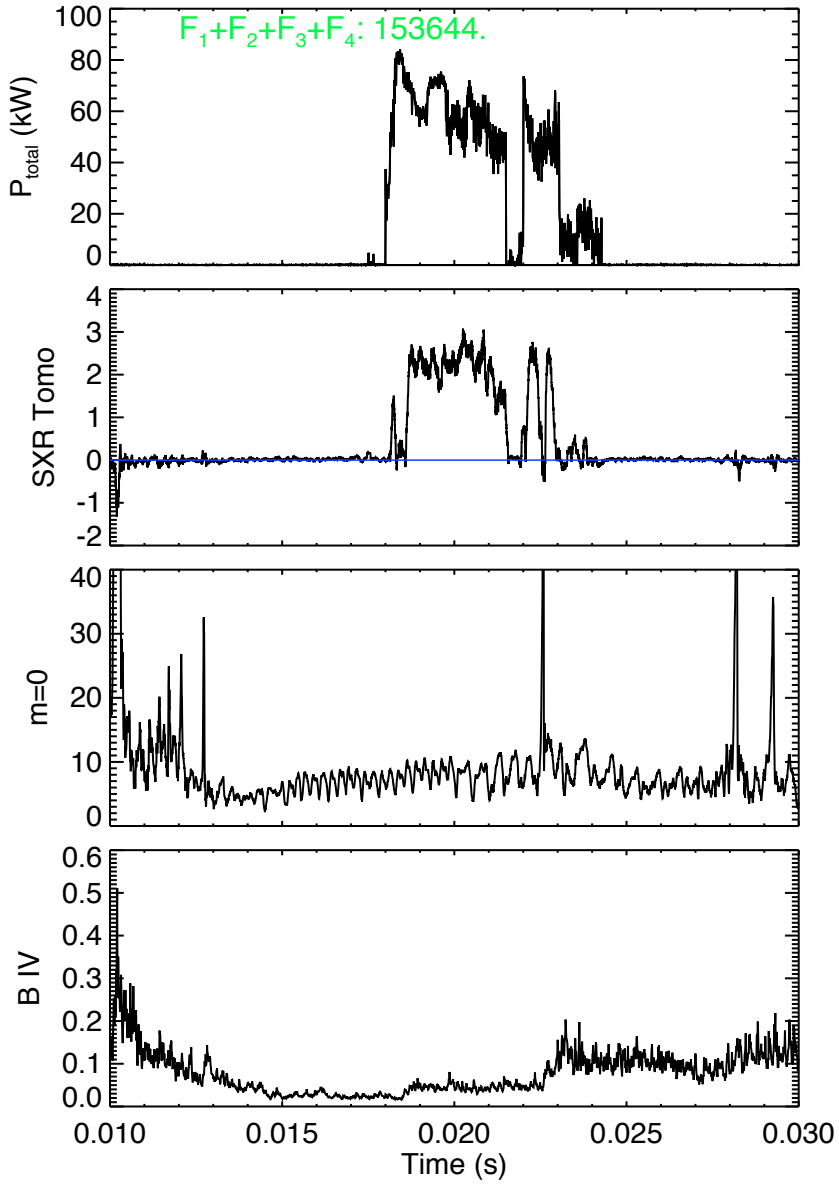

FIG. 2. Injected RF causes an increase in SXR emission in the absence of m=0 activity. Boron emission is also enhanced by rf.

until a loss of confinement as indicated by the m=0 burst at 22.5 ms. At this time, the SXR signal again vanishes quickly; in fact here the SXR signal goes through zero to a negative value. This is a real effect. This photodiode-based diagnostic produces a positive signal for the real photocurrent caused by SXR emission incident on the semiconductor (photocurrent is in the 'reverse bias' direction associated with a diode). A diode is also the fundamental part of a crystal rf detector: in this application it acts as a rectifier (current in the 'forward bias' sense); rf pickup in this system opposes the real emission signal. This is illustrated at the point in time where SXR emission is lost due to poor confinement and rf injection is ongoing.

These data are consistent with the target scenario: the launched X-mode converts to the Bernstein mode and propagates to the doppler-shifted cyclotron resonance. However, due to complicated impurity source behavior during the rf injection, the mechanism leading to the SXR emission has not been experimentally identified.

Positive results of EBW experiments on MST have motivated a large effort to increase the available source power. A 1 MW 5.5 GHz klystron has been procured as an rf power source for the next step in the experimental development. This choice of frequency is based on a number of factors. Ray tracing studies demonstrate that this frequency is nearly optimal for MST discharges of modest toroidal current, and the availability of the rf source was indeed a factor. The klystron has been tested on the bench at short (4μs) pulse length, and a power supply for a 10 ms pulse is nearing completion, with antenna coupling and heating experiments to commence thereafter.

3. Lower Hybrid

Theoretical feasibility and optimization studies have identified the lower hybrid slow wave as a good candidate for current density profile control in the RFP [6]. This wave is complementary to EBW in that the accessibility physics is more developed, but the antenna is more challenging. Ray tracing and Fokker-Planck calculations have identified suitable propagating waves that can provide localized current drive with relatively high current drive efficiency. These theoretical studies show that the location of the driven current can be controlled by choice of parallel wave number and rf frequency, and the predicted efficiency of current drive is sufficient for suppression of MHD tearing modes at 1-2 MW of injected power.

Numerical modeling has identified 800 MHz as a reasonable frequency for launching the slow wave at the MST boundary, and predicts efficient off-axis current drive. An interdigital line antenna has been successful to the transmitter power limit, which currently stands at about 100kW of launched power. The antenna is a slow wave structure, with $N_{||} \sim 7.5$, and has an rf feed on each end. Power is delivered to one end of the antenna, travels along the structure and radiates, and the remaining power is fed out at the opposite side of the antenna. Interchanging the input and output ports reverses the direction of the target wave launch, and hence is a way to attempt co- and counter- current drive experiments.

As the lower hybrid wave alters the electron distribution by pulling out a high-energy tail, measurements of xray flux are key to understanding the experiments. Hard x-rays have been generated when power is fed in either direction through the antenna. The energies of the HXRs

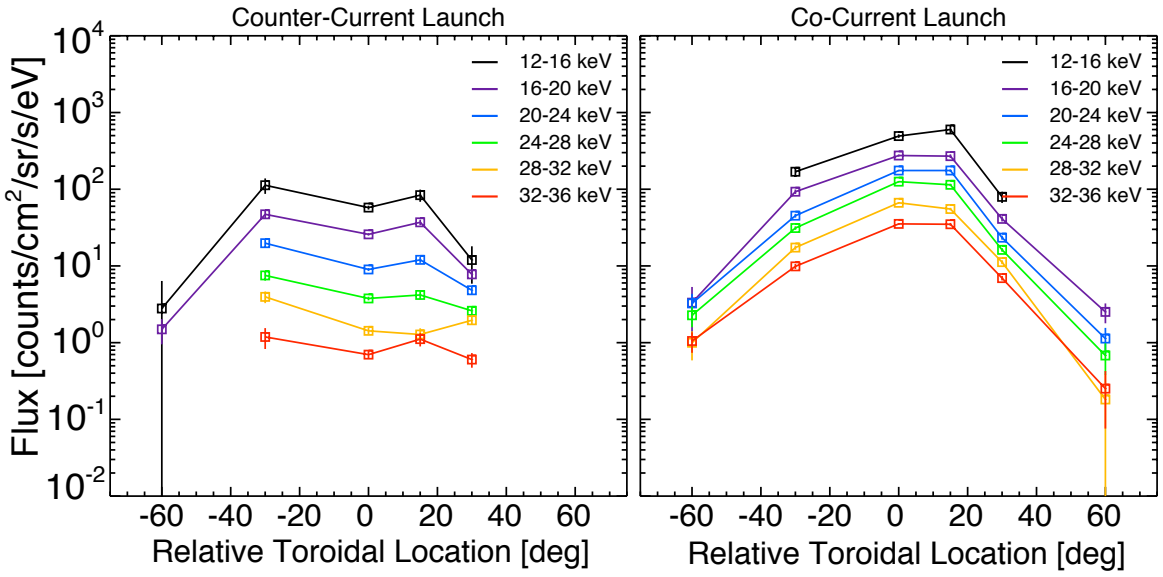

FIG. 3. HXR falls off with toroidal angle, asymmetrically.

produced are up to 50 keV which is $\sim$ 10 times the estimated rf potential in front of the antenna rods and greater than that of the $\sim$4 keV electrons resonant with the wave at $N_{||}$ = 7. An interesting feature of the emission is that it is toroidally localized for both counter- and co-current launch [7], as seen in Fig. 3. HXRs are only observed above background levels up to 60 degrees away toroidally from the antenna location. Very little emission is seen when the detector is 90 degrees away from the antenna. The flux observed for the same antenna power and plasma conditions is an order of magnitude higher for co-current versus counter-current launch. There is also a slight toroidal asymmetry in the flux about the antenna location.

In a separate xray survey experiment, an array of detectors was used to view directly the active antenna [7]. The results of this survey are shown in Fig. 4. There is much higher flux from the end of the antenna into which power is fed. This higher flux is inconsistent with bremsstrahlung from fast electrons produced by waves in the plasma. However, because the power distribution along the antenna structure has an exponential fall-off, these observations could be consistent with interaction of electrons with the near-field of the antenna. To test this hypothesis, a Monte Carlo test-particle code was developed to calculate the electron distribution after interaction with the near-field of the antenna [7]. The inputs to the code are the edge plasma parameters, e.g., temperature and magnetic field (magnitude and pitch), and rf power. The results show that a perpendicular tail in the electron distribution is pulled out to energies of $\sim$40 keV. In addition, there is higher flux for the co- versus the counter-current launch direction. Both of these results are consistent with the measured HXR profiles. The flux can also be affected by changing the pitch of the magnetic field that intersects the antenna. This can help explain the slight asymmetry seen in the toroidal profiles.

A third xray survey experiment has focused on lower energy xray emission; this is a somewhat more difficult measurement in that there is an appreciable background flux in the absence of LH injection. Fig. 5 is a demonstration that there is an LH induced SXR enhancement as well: the 2-10 keV diagnostic shows an order of magnitude higher flux at 10keV with rf than without.

Detailed analysis of all xray measurements include comparison to Fokker-Planck calculations.

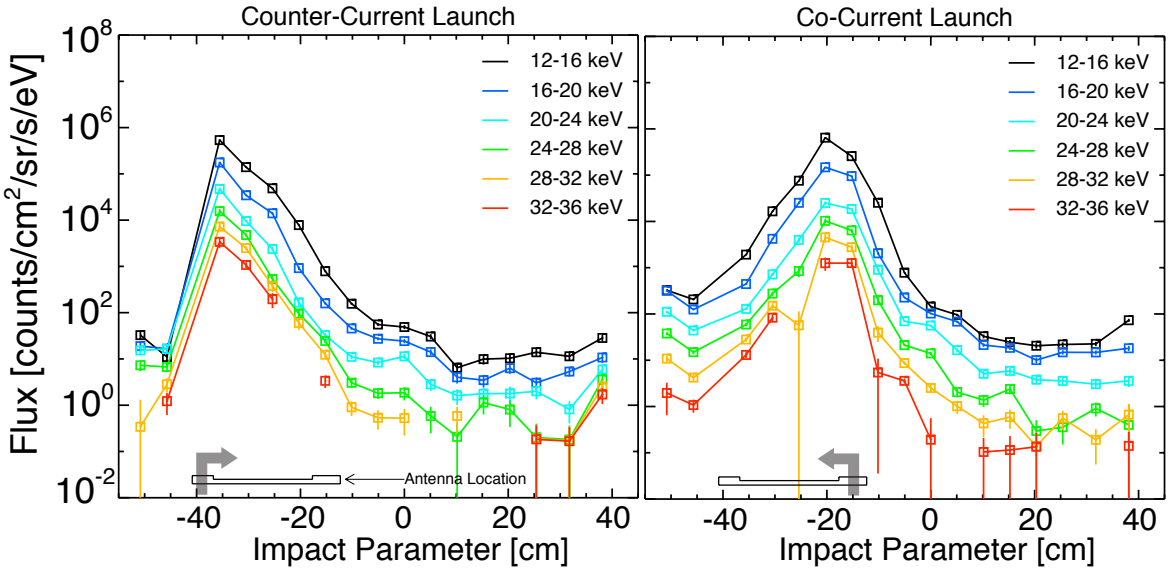

FIG. 4. HXR flux measured in antenna near field for co- and counter- injection tests.

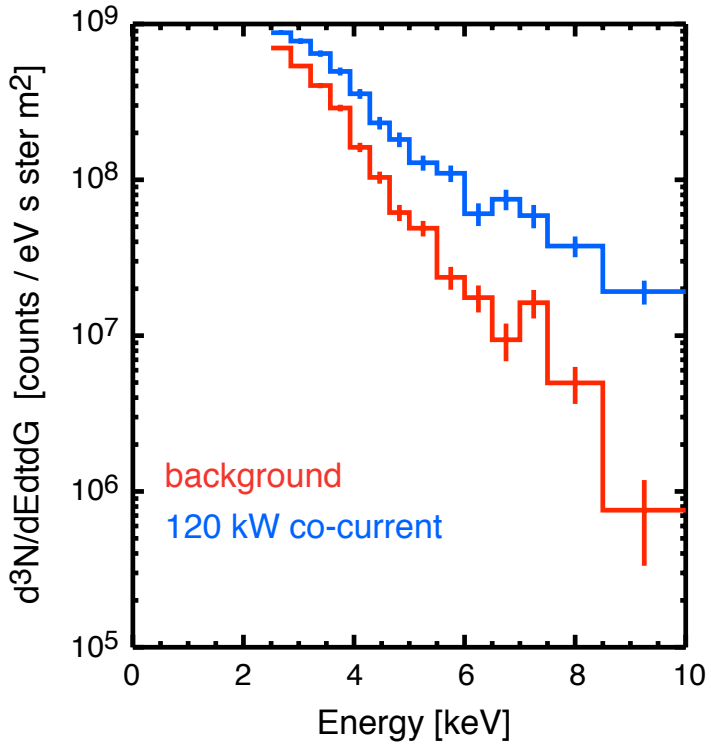

FIG. 5. SXR emission enhanced during LH injection. The SXR diagnostic is located toroidally near the antenna.

This has been a difficult problem (numerically) due to the high diffusivity of the RFP plasma. Recent improvements to the Fokker-Planck calculation have enabled more accurate comparisons with experiment and further calculations are pending. The primary challenge facing LH current drive on MST is devising a system which extends the source power up to greater than 1 to 2 MW. Exploration of different antenna types and source availability is underway.

4. Summary

Two rf-based current drive schemes are under development on MST. Lower hybrid current drive, a proven technique in tokamaks, has tremendous engineering restrictions for use on the RFP. A successful antenna concept has been constructed, and clear interaction of electrons with electric field of the antenna is observed. Electron Bernstein waves are being pursued as an alternate method of heating and driving current in the overdense RFP plasma. In experiments with about 100kW of source power a localized increase of SXR (4-7 keV) emission is observed in high confinement regimes of the MST discharge. Extension to 1MW source power is underway and initial experiments to test antenna power handling limits are under design.

This work is supported by USDOE.

References

[1] H. P. Laqua, V. Erckmann, H. J. Hartfuss, H. Laqua, *Phys Rev Letters* **78** 18, 3467, (1997).

[2] A. Mueck, L. Curchod, Y. Camenen, S. Coda, T. P. Goodman, H. P. Laqua, A. Pochelon, L. Porte, F. Volpe, *Phys Rev Letters* **98** 17, 175004, (2007).

[3] V. Shevchenko, G. Cunningham, A. Gurchenko, E. Gusakov, B. Lloyd, M. O'Brien, A. Saveliev, A. Surkov, F. Vole, M. Walsh, *Fus Sci Tech* **52** 2, 202, (2007).

[4] P. K. Chattopadhyay, J. K. Anderson, T. M. Biewer, D. Craig, C. B. Forest, R. W. Harvey, A. P. Smirnov *Phys. Plasmas* **9**, 3, 752 (2002)

[5] M. Cengher, J. K. Anderson, C. B. Forest, V. Svidzinski, *Nuc. Fusion* **40**, 521 (2006)

[6] E. Uchimoto, M. Cekic, R. W. Harvey, C. Litwin, S. C. Prager, J. S. Sarff, and C. R. Sovinec *Phys. Plasmas* **1**, 3517 (1994)

[7] M. C. Kaufman, Ph.D. thesis, University of Wisconsin-Madison, 2009.